Evaluation of PIC 181 and Mn:PIN-PMN-PT thickness extensional rings for use in power ultrasonic devices for minimally invasive surgery

Nicola Giuseppe Fenu, Xuan Li
Margaret Lucas and Sandy Cochran
Centre for Medical and Industrial Ultrasonics
James Watt School of Engineering
University of Glasgow, G12 8QQ, UK
Email: nicola.fenu@glasgow.ac.uk

***Abstract*—High-Q PIC 181 hard piezoceramic and high-k Mn:PIN- PMN-PT piezocrystal thickness extensional rings have been compared for use in the actuation of an ultrasonic scalpel for robotic endo-surgery. Measured material properties have been verified with both finite element analysis and laser vibrometry, to assess the materials' suitability for high power devices. Measured material properties have been verified with both finite element analysis and laser vibrometry, to assess material's suitability for high power devices. Measurements have shown a $k_t = 0.25$ and $Q_m = 2200$, and $k_t = 0.62$ and $Q_m = 1100$, for PIC 181 and Mn:PIN-PMN-PT respectively. Conventional bolted Langevin-style transducers (BLTs) have been successfully designed and built to resonate at 20 kHz for both piezomaterials. Modal parameters and performance have been modelled in FEA and measured via laser doppler vibrometry. When devices were excited with 50 V_{rms} at L1 a displacement of 8 μm and 7 μm was measured for PIC-181 and Mn:PIN-PMN-PT BLTs respectively. Results suggest that a similar resonant frequency can be achieved with a shorter and equally functional device excited by Mn:PIN-PMN-PT piezocrystals.**

I. Introduction

ROBOTIC endo-surgery is becoming more and more popular in minimally invasive procedures. In order to facilitate further progress, smaller ultrasonic scalpels are required, allowing access through a burr hole, typically 10 - 14 mm in diameter, or laparoscopic port, 5 mm or 10 mm in diameter. Normally, these tools employ a rigid wave guide to transfer the vibration inside the human body from a Langevin-type transducer fixed on a robotic arm. The transducer is axially constrained with the robot and only limited movement is permitted. In order to enable more degrees of freedom at the end effector, the transducer should be attached to a wristed joint to replicate the experience of open-surgery [1]-[3]. Currently this is not achievable if rigid waveguides, and materials conventionally used in ultrasound, are adopted. Mn:PIN-PMN-PT single crystals are emerging as a potential material for use in high power ultrasonics applications, due to their simultaneously high piezoelectric coefficient (d_{ij}), electromechanical coupling (k_{ij}), and mechanical quality factor (Q_m) [4][5]. When higher efficiency and lower electromechanical losses are taken into account, these materials may allow realisation of smaller devices, better suited for use via a burr hole or port. To contribute to understanding of the potential performance gain, hard piezoceramic (PIC 181, PI Ceramics, Lederhose, Germany) and new Mn:PIN-PMN-PT piezocrystal (TRS Technologies, PA, USA) rings are compared in actuating a simple, cylindrical 20 kHz half-wavelength resonator, presently without introducing complex horn geometries and gain profiles.

This work was supported by *Ultrasurge, Surgery Enabled by Ultrasonics*, funded by the Engineering and Physical Sciences Research Council (EPSRC), EP/R045291/1.

II. Materials and Methods

A. Piezoelectric Material Characterisation

Table I presents a comparison between material properties provided by the manufacturer and those obtained via measurements, curve-fitting (PRAP, TASI Technical Software Inc., Kingston), and finite element analysis (FEA-OnScale, Glasgow, UK). Impedance measurements have been taken by a calibrated custom fixture for an impedance analyser (Agilent 4294, Keysight Technologies, Santa Rosa, CA, USA), and d_{33} measurements by using a Berlincourt meter (Model ZJ-6B, Institute of Acoustic, Chinese Academy of Sciences, Beijing, China). A total of two rings (outer diameter 10 mm, inner diameter 5 mm, and thickness 2 mm) were used for material characterisation for each material, PIC 181 and Mn:PIN-PMN-PT.

The frequency in Hz of the thickness extensional mode of a ring is given by Equation 1 [6], where t is the thickness of the ring, ρ is the density and s_{33}^D is the elastic compliance at constant electric field.

$$F_{r-TE} = \frac{1}{2t\sqrt{(\rho s_{33}^D)}} \tag{1}$$

Fig. 1 shows the comparison between the resonance frequency of the thickness mode obtained via Equation 1 and via FEA as a function of ring thickness for both materials. The full set of material properties was provided by the manufacturer for

TABLE I
MATERIAL PROPERTIES OF PIC 181 AND MN:PIN-PMN-PT RINGS

	Fs (MHz)	**Z** (Ω@Fs)	$\mathbf{d_{33}}$ (pC/N)	$\mathbf{k}_t$	$\mathbf{k_{33}}$	$\mathbf{Q}_m$	ϵ^S_{33} (rel.)
PIC 181							
Data Sheet	/	/	253	0.46	0.66	2200	624
Measurement	1.11	4	290	0.25	0.26	2200	/
PRAP	1.11	/	/	0.29	/	/	620
FEA	1.09	6.3	/	0.27	0.28	1500	/
Mn:PIN-PMN-PT							
Data Sheet	0.55	/	/	0.66	0.94	/	/
Measurement	0.55	6.0	860	0.62	0.80	1100	/
PRAP	0.57	/	/	0.62	/	/	800
FEA	0.51	22.2	/	0.66	0.88	450	/

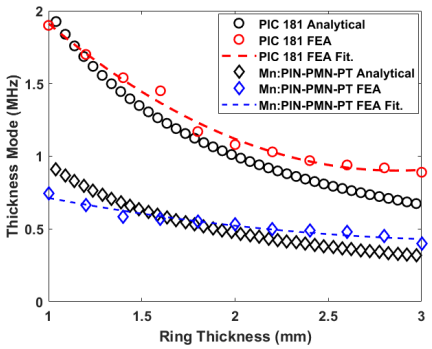

Fig. 1. Thickness mode Analytical vs FEA.

PIC 181, whereas, for Mn:PIN-PMN-PT, properties obtained through single-sample characterisation were used [7]. A comparison between measured and simulated electrical impedance magnitude, used to calculate the properties presented in Table I, is shown in Fig. 2 for both materials. To complete the characterisation, Laser Doppler vibrometry (LDV, OFV 534, Polytec Ltd., Waldbronn, Germany) was used. As shown in Fig. 3 the thickness mode observed in FEA was validated via mode shape reconstruction. By laser-scanning the electroded top surface of the ring, the maximum displacement and phase response were recorded at each point for a mesh of 100 x 100 points with x 0.1 mm mesh size. The samples were both excited with a 3 V_{PP} sine wave at their resonance frequency and a total of 25 measurements were taken at each point. The displacement of the top electroded surface was also measured between 0-10 V_{PP} for both PIC 181, shown in Fig. 4(a), and Mn:PIN-PMN-PT Fig. 4(b).

B. Observations for high power ultrasonics

PIC 181 and Mn:PIN-PMN-PT rings have shown different characteristics. By considering material properties only, the piezoceramic shows higher Q_m, and lower d_{33} and k_{33} than the Mn:PIN-PMN-PT sample. Moreover, the resonance frequency for the thickness extensional mode (TE) of PIC 181 is double that for the TE mode in the Mn:PIN-PMN-PT sample, due to the higher elastic compliance of piezocrystals compared to piezoceramics. This also leads to the fact that when targeting a specific device frequency (e.g. 20 kHz), the device in which piezocrystals are embedded will be considerably shorter than a piezoceramic-based device. The vibrational frequency also

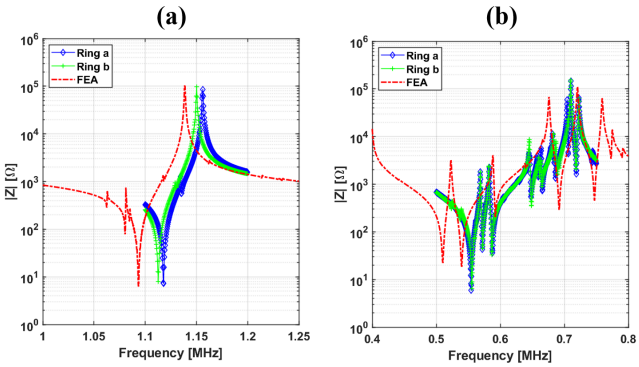

Fig. 2. Electrical impedance magnitude of **(a)** PIC 181, and **(b)** Mn:PIN-PMN-PT thickness extensional mode rings.

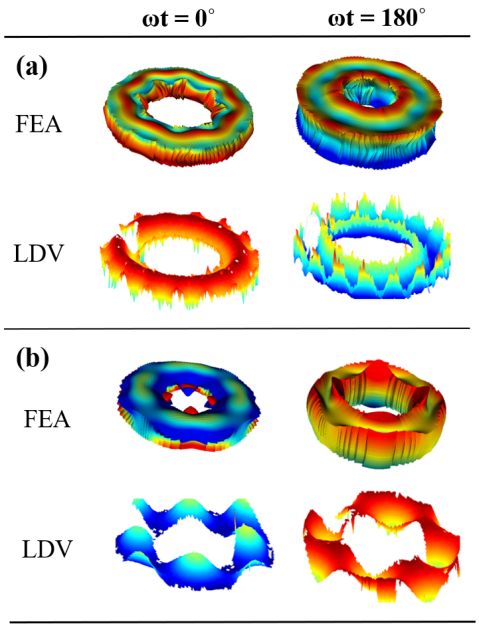

Fig. 3. Comparison between vibrational mode shapes obtained via FEA and Laser Doppler Vibrometry at resonance frequency for **(a)** PIC 181, and **(b)** Mn:PIN-PMN-PT thickness extensional mode rings. All amplitude indications are in normalized arbitrary units.

affects the vibration amplitude, as shown in Fig. 4, where the crystals show higher surface displacement and wider bandwidth at resonance. A difficulty is that the measured and simulated electrical impedance, Fig. 2(b), and mode shape, Fig. 3(b), of the Mn:PIN-PMN-PT ring appear to be coupled with other modes. However, unwanted modes are predicted to be suppressed under the prestress conditions found in power ultrasonics devices.

C. Device Modelling, Assembly and Methods

The device configuration used for this work is a standard bolted Langevin-style transducers (BLT), consisting of two metal (titanium 6Al-4V Grade 5 alloy) end-masses sandwiching a pair of PIC181 or Mn:PIN-PMN-PT rings for excitation held together by means of a pre-stress bolt made from tool

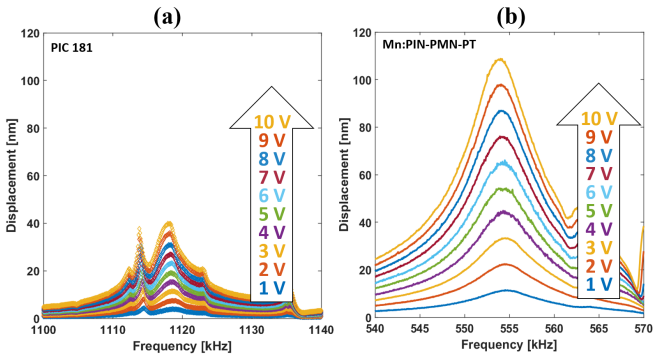

Fig. 4. Measured displacement of **(a)** PIC 181, and **(b)** Mn:PIN-PMN-PT thickness extensional mode rings.

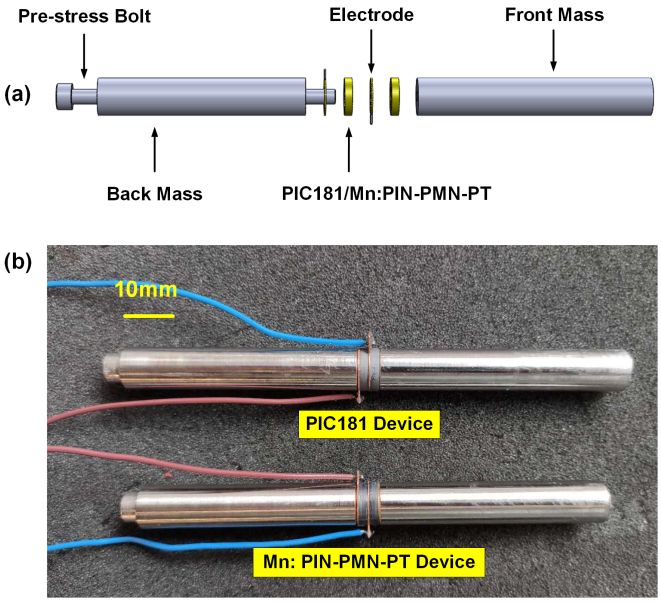

Fig. 5. **(a)** Exploded view of a BLT bar device **(b)** Titanium 20 kHz half-wavelength resonators embedding: PIC 181, and Mn:PIN-PMN-PT thickness extensional mode rings.

steel. An exploded view of these components is presented in Fig. 5(a) with the dimensions of each component presented in Table II. In the present work, the length of the end-masses is tuned to enable the device to operate primarily at its first longitudinal mode of a half-wavelength at approximately 20 kHz. The fabricated BLT devices are presented in Fig. 5(b). They were modelled in Abaqus computer-aided engineering (CAE SIMULA, Dassault Systèmes, RI, USA) to obtain both modal and electrical parameters. During assembly, the components were pre-stressed using a bolt, following guidelines for achieving a stable response of the transducer without risking depolarisation [8], [9].

For the PIC181 device, with an applied pre-stress in the recommended region of $<$ 30 MPa [11], the applied torque was calculated to be no more than 3.0 Nm. For the Mn: PIN-PMN-PT device a torque of 1.5 Nm, half of that for the PIC181 device, was applied to ensure sufficient contact between the crystal and the end-masses whilst avoiding any possibility

TABLE II
MODELLED AND FABRICATED PARTS OF **A**: PIC 181, AND **B**: MN:PIN-PMN-PT DEVICES

Material	**Back Mass** Ti6Al4V (mm)	**Front Mass** Ti6Al4V (mm)	**M4 Bolt** Steel (mm)
a			
Fabricated	53	57	65
Abaqus FEA	55	62	70
b			
Fabricated	49.5	52	65
Abaqus FEA	52	56	65

of damage. The impedance spectra of the devices at their final torque levels were recorded. To capture the mechanical characteristics of the devices, experimental modal analysis (EMA) was performed, to allow validation of the design of the devices in FEA. EMA was performed by measuring frequency response functions (FRFs) from which the modal parameters, i.e. frequency, damping, and mode shape, were extracted [10]. To study the vibration responses of the BLTs in resonance at higher excitation levels, harmonic response experiments were performed. These were executed through a range from below to above the resonance frequency of the L1 mode using a burst sine signal and the longitudinal vibration response was measured using a 1-D laser Doppler vibrometer (OFV 303, Polytec Ltd.,Waldbronn, Germany) at the BLT front face. A 3 s gap in time between two burst excitations was applied to ensure dissipation of heat generated in the devices, avoiding any consequent effects.

III. RESULTS

The complex impedance spectra of the BLTs are presented in Fig. 6 and Table III shows modelled and measured device parameters. The Mn:PIN-PMN-PT device exhibits a wider bandwidth, and as a comparison, the peak of the resonance of the PIC181 device shows a sharper characteristic which implies a higher Q_m. The effective electromechanical coupling coefficients, k_{eff}, and Q_m for both BLTs were calculated and are presented in Table III. Fig. 7 shows the waveforms predicted in FEA and measured in EMA of mode L1 of the BLTs. Simulation and experiment present good agreement in terms of the location of the displacement nodes, maximum amplitudes, and ratios of vibration amplification. The discrepancies in the resonance frequencies of the devices between prediction and measurement are 1.1% and 0.13% for the PIC181 and Mn: PIN-PMN-PT devices, respectively.

Fig. 8 shows the vibration characteristics of both devices, using excitation voltages ranging from 1 V_{rms} to 50 V_{rms}, with an increment of 10 V_{rms}. Clearly, as the applied voltage increases, the vibration amplitude increases, with a maximum 8 μm amplitude achieved at the end face of the PIC181 device at 50 V_{rms}. A slightly lower amplitude of 7 μm is reached for the Mn:PIN-PMN-PT device. Another observation is that the shift in the resonance frequency is considerably larger for the Mn:PIN-PMN-PT device than the PIC181 device.

TABLE III
BLTs Modelled and Measured Parameters

	Fs (kHz)	Z (Ω@Fs)	k_{eff}	Q_{eff}	Torque (Nm)
PIC 181 Device					
Measurement	20.410	644.7	0.164	547	3.0
Abaqus FEA	20.103	1302.1	0.156	600	/
Mn:PIN-PMN-PT Device					
Measurement	20.265	283.3	0.341	163	1.5
Abaqus FEA	20.273	728.4	0.380	148	/

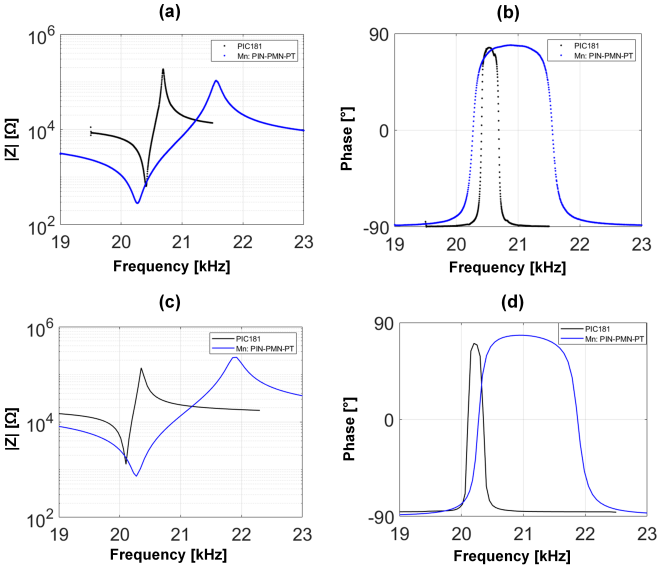

Fig. 6. Simulated and measured electrical impedance and phase of the BLT devices, **(a)** and **(b)**: experiments, **(c)** and **(d)**: Abaqus simulation.

IV. Conclusion and Future Work

The use of Mn:PIN-PMN-PT rings allowed us to build a BLT that is 9 mm shorter than the equivalent using PIC181 rings, confirming it as a potential candidate to achieve our goal to aid surgery by minimizing tool length. No major limitation and/or great advantage was observed in the use of Mn:PIN-PMN-PT with regard to the L1 vibration response. The piezocrystal-based device, however, appears to have a higher bandwidth and it exhibits a larger resonance frequency shift using the same applied voltage amplitude. Further investigation will focus on the higher harmonic modes and their vibration response at higher resonance frequencies. Moreover, the temperature rise during high power excitation conditions will be monitored for both materials; this may be a major risk for Mn:PIN-PMN-PT piezocrystals, with a phase transition temperature of approximately 100°C. In addition, electrical impedance matching networks between the energy source and the transducers will be considered to optimise the energy transmission efficiency of the BLTs.

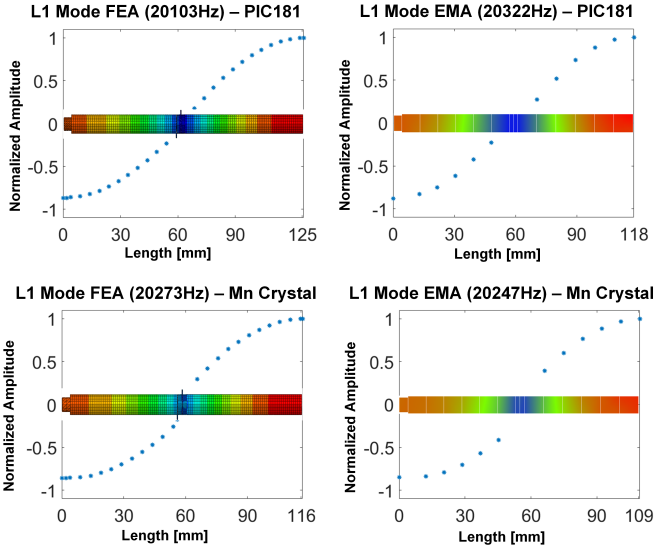

Fig. 7. Extracted vibration modeshapes of FEA and EMA analyses. All amplitude indications are in normalized arbitrary units.

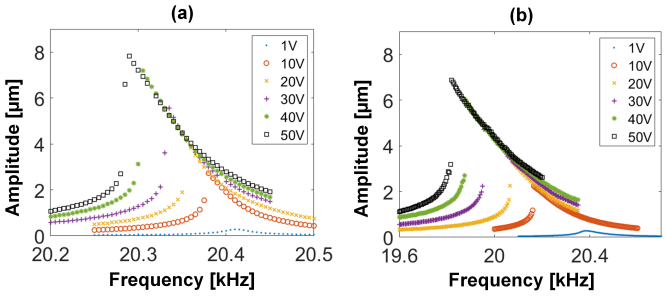

Fig. 8. Vibration characteristics of the BLT devices: **(a)** PIC181 device **(b)** Mn:PIN-PMN-PT device.

References

[1] M. Kroh, *"Essentials of Robotic Surgery"*, M.Kroh S. Chalikonda Ed. Springer, Switzerland, 2015. DOI: https://doi.org/10.1007/978-3-319-09564-6.

[2] G. Spinoglio, *"Robotic Surgery Current Applications and New Trends.* G.Spinoglio Ed. Springer-Verlag, Switzerland, 2015. DOI: https://doi.org/10.1007/978-88-470-5714-2.

[3] Yang, S. C., Ahn, J., Kim, J. H., Yi, J. W., Hur, M. H., Lee, K., "Comparison of the vessel sealer Extend with harmonic ACE in robotic bilateral axillary-breast approach thyroid surgery", *Gland Surgery*, vol. 9, no. 2, pp. 164-171, 2020. DOI: https://doi.org/10.21037/gs.2020.01.18

[4] Zhang, S., Li, F., Jiang, X., Kim, J., Luo, J., Geng, X., "Advantages and challenges of relaxor-PbTiO3 ferroelectric crystals for electroacoustic transducers. A review", *Progress in Materials Science*, no. 68, pp. 1–66, 2015. DOI: https://doi.org/10.1016/j.pmatsci.2014.10.002

[5] Zhang, S., Shrout, T. R., "Relaxor-PT single crystals: Observations and developments", *IEEE T-UFFC*, vol. 57, no. 10, pp. 2138–2146, 2010. DOI: https://doi.org/10.1109/TUFFC.2010.1670

[6] Evan, M., Kihiu J., Nyakoe G., Mutuli S., Kimotho J., "Determination of resonant frequency of a piezoelectric ring for generation of ultrasonic waves", *Innovative Systems Design and Engineering*, vol. 2, no. 4, pp. 103–111, 2011.

[7] Fenu N.G., Giles-Donovan N., Sadiq M., Cochran S., "Progress Towards Piezocrystal and Pb-Free Piezoceramic Performance Prediction for High Power Ultrasound Device", *IEEE-IUS*, Kobe, Japan, 2018.

[8] Kim, J., Lee, J., "Parametric study of bolt clamping effect on resonance characteristics of langevin transducers with lumped circuit models", *Sensors*, vol. 20, no. 7, pp. 1–9, 2020.

[9] Choi, C., Seo I. t., Song D., Jang M. S., Kim B. Y., Nahm S., Sung T. H., Song H. C., "Relation between piezoelectric properties of ceramics and output power density of energy harvester", *Journal of the European Ceramic Society*, vol. 33, no. 7, pp. 1343–1347, 2013.

[10] Avitabile, P. "Experimental Modal Analysis", *Sound Vib.*, vol. 35, no. 1, pp. 1–15, 2001.

[11] DeAngelis, D. A., Schulze, G. W., Wong, K. S., "Optimizing Piezoelectric Stack Preload Bolts in Ultrasonic Transducer", *Physics Procedia*, vol. 63, pp. 11–20, 2015.